Thirty Years of Gipps' Car-Following Model

3 authors:

Biagio Ciuffo
European Commission
46 PUBLICATIONS   **783** CITATIONS

SEE PROFILE

Vincenzo Punzo
University of Naples Federico II
48 PUBLICATIONS   **1,037** CITATIONS

SEE PROFILE

Marcello Montanino
University of Naples Federico II
18 PUBLICATIONS   **480** CITATIONS

SEE PROFILE

Some of the authors of this publication are also working on these related projects:

TESYS Rail - techniques and tools to increase the environmental sustainability of rail transport systems View project

FERSAT - Study of a railway signaling system based on the innovative use of satellite technologies and their integration with terrestrial technologies View project

Thirty Years of Gipps' Car-Following Model
Applications, Developments, and New Features

Biagio Ciuffo, Vincenzo Punzo, and Marcello Montanino

Researchers and practitioners commonly use car-following models for road traffic studies. Although dozens of models have been presented so far, the one proposed by Peter G. Gipps in 1981 is still one of the most extensively used. However, many features of the model are still not well known or neglected in common applications. In this context, the current study summarizes and analyzes the main findings available in the scientific literature for the Gipps' car-following model and introduces some of its novel features that may improve its capability to reproduce real trajectory data. In particular, the structure of the acceleration component of the model is analytically investigated for what concerns the meaning of some parameters that in common practice are usually kept to some empirically derived fixed values. Possible versions of Gipps' model are presented, and their performance to reproduce real vehicle trajectories is evaluated and compared. The results achieved show the necessity for these parameters to be calibrated to improve the model's predictive capabilities.

In 1981, P. G. Gipps published a study titled "A Behavioural Car-Following Model for Computer Simulation" (*1*). This paper was bound to have a considerable impact on traffic flow theory and practice, and the model described became widely recognized as the Gipps' car-following model.

Car-following models try to explicitly reproduce the complex dynamics governing the actions of the driver–vehicle system while the driver is following another vehicle. Dozens of car-following models had been presented previously and new ones are continuously being proposed; since an up-to-date comprehensive review is not available, the reader can refer to various sources presenting a clustered review of the topic (*2–4*). Different assumptions have been presented on the strategy adopted by a driver–vehicle system to adapt its speed to the presence of a vehicle downstream moving in the same direction.

Car-following models have two main applications: modeling macroscopic traffic propagation and evolution and modeling the microscopic behavior of the driver–vehicle system during follow-the-leader activity. In the first case, car-following models are usually included within a broader modeling framework of traffic micro-simulation (acting as the main driver for the vehicles' movements) and the main aim is to simulate and appraise the effect of introducing political and technological measures to mitigate the impact of road traffic on society. In the second case, car-following models are mainly used in the design of devices working onboard the vehicles to assist drivers to maintain safe and comfortable driving conditions (e.g., intelligent speed adaptation systems, and collision avoidance systems).

The high number of car-following models proposed could be motivated by their overall incapability to reproduce both traffic propagation and driver–vehicle interactions without relying on the overfitting produced by their parameters, which are usually unnecessary and without a clear physical interpretation (this difficulty certainly poses serious concerns about the models' capability to reproduce unpredictable conditions). As a result, most of the applications using car-following models usually adopt the less recent, "classical" models. The Gipps' car-following model is one of them.

Reasons for the fascination with the Gipps' model primarily reside in the clear physical context that the author adopted to derive it: a driver adapts his speed in order to smoothly reach the desired speed or to safely proceed behind his leader. In addition, Wilson (*5*) demonstrated that, similar to other "reductionist models" like that of Bando et al. (*6*), the Gipps' model may also allow for a uniform flow of traffic to lose stability for certain ranges of its parameters. Stability loss is an important feature since it allows for typical traffic mechanisms to be produced (such as flow breakdown and spontaneous traffic jam formation).

However, as noted by Ranjitkar et al. (*7*) and Spyropoulou (*8*), some properties of the Gipps' model have been hidden by the positions assumed by Gipps himself and thus the scope of the model might even be enlarged.

For all these reasons, in this study the main features of the Gipps' car-following model as they have been derived in different studies and applications are summarized. Furthermore, some analyses are presented that were performed on the acceleration component of the Gipps' model, providing some insight on the effect that the relaxation of three parameters, usually considered as fixed, may have on the overall model performance.

At the end of the analysis different versions of the Gipps' model as derived from the literature review and the analyses carried out will be compared. The comparison is made possible by calibrating and validating the different versions in order for them to reproduce vehicle trajectory data.

ORIGINAL FORMULATION

The Gipps' car-following model is the most commonly used model pertaining to the class of "safety distance" or "collision avoidance" models. Models of this class aim to specify a safe following distance and to adapt the driver's behavior in order to always keep the distance. The basic idea behind the model is that each driver plans his or her speed for the following instant (i.e., after a delay τ) such that he or she can safely stop even in the event of the leading vehicle's sudden

B. Ciuffo, Institute for the Environment and Sustainability, and V. Punzo, Institute for Energy and Transport, Joint Research Centre, European Commission, Via E. Fermi, 2749–21027 Ispra (VA), Italy. M. Montanino, Department of Transportation Engineering, Università di Napoli Federico II, Via Claudio, 21–80125 Napoli (NA), Italy. Corresponding author: B. Ciuffo, bciuffo@unina.it.

braking. In case the driver has no vehicles in front, speed planned for time $(t+\tau)$ is obtained from an inequality of experimental origin that combines two conditions: (a) that the speed never exceeds the driver's desired speed and (b) that acceleration decreases with increasing speed till it becomes null when the desired speed has been reached.

According to the Gipps' model, the speed attained by a vehicle at a given time instant $(t+\tau)$ [in which the delay τ is the "apparent" driver's reaction time (1)] is given by

$$\dot{s}_f(t+\tau) = \min\left\{\dot{s}_{f,\text{acc}}(t+\tau), \, \dot{s}_{f,\text{dec}}(t+\tau)\right\} \tag{1}$$

where

$$\dot{s}_{f,\text{acc}}(t+\tau) = \dot{s}_f(t) + 2.5\ddot{S}_f\tau\left(1 - \frac{\dot{s}_f(t)}{\dot{S}_f}\right)\sqrt{0.025 + \frac{\dot{s}_f(t)}{\dot{S}_f}} \tag{2a}$$

$$\dot{s}_{f,\text{dec}}(t+\tau) = b_f\tau + \sqrt{b_f^2\tau^2 - b_f\left[\begin{array}{c}2\left(s_l(t) - s_f(t) - \left(L_l + \Delta S^0\right)\right) \\ -\dot{s}_f(t)\tau - \dfrac{\dot{s}_l^2(t)}{\hat{b}}\end{array}\right]} \tag{2b}$$

where

f, l = follower and leader, respectively;
s = space traveled by vehicle;
$\dot{s}$ = vehicle's speed;
$\dot{S}_f, \ddot{S}_f$ = follower's maximum desired speed and maximum acceleration, respectively;
$b_f, \hat{b}$ = respectively, most severe braking that driver of following vehicle wishes to undertake and his estimate of leader's most severe braking capabilities (in current formulation they are considered with their sign);
L = leader's vehicle length; and
ΔS^0 = intervehicle spacing at a stop.

In practice, the driver chooses the minimum speed between two possible alternatives, where the first ($\dot{s}_{f,\text{acc}}$) accounts for the driver's willingness to reach his desired speed, whereas the second ($\dot{s}_{f,\text{dec}}$) aims to preserve a safe distance behind the leader.

In the model derivation, Gipps considered an additional term, θ (an additional comfort delay in the braking component of the model), in the analytical derivation of the model to allow the follower not to brake always at his or her maximum desired rate. Gipps then assumed for θ to be equal to $\tau/2$, and for this reason it does not appear in Equations 2a and 2b. In fact, Gipps proves that in the case $\theta = \tau/2$ and $b_f > \hat{b}$—that is, the willingness of the preceding driver to brake hard has not been underestimated—a vehicle traveling at a safe speed would be able to maintain a safe speed and distance indefinitely. Indeed, the relative magnitude of braking rates b_f and $\hat{b}$ is the cornerstone for model stability. As shown successively by Wilson, $b_f > \hat{b}$ is a sufficient condition for the linear stability of the model.

APPLICATIONS AND ANALYSES

As already pointed out, the Gipps' car-following model is one of the most widely used models in both research applications and practice. In particular it represents the building block for different microscopic traffic simulation software programs, such as AIMSUN (9), DRACULA (10), SISTM (11), SIGSIM (12), and SITRAS (13). This fact means that it is used daily by thousands of practitioners

without their realizing it and for every kind of traffic application. It is beyond the aim of the current paper to provide details on the practical applications in which the models or the previous software has been used. On the contrary, the intent here is to summarize the way the Gipps' model is implemented in the different software or research applications in order to understand potential benefits deriving from the experience in their development.

The work of Wilson represents the most complete analysis of the Gipps' model (5). He found equilibrium solutions of the model for uniform flow in the form of steady-state solutions of the system of equations given by Equation 3 and by the equation describing the evolution of space headways. Indeed, making explicit the value of θ, Equation 2b becomes

$$\dot{s}_{f,\text{dec}}(t+\tau) = b_f\left(\frac{\tau}{2} + \theta\right)$$
$$+ \sqrt{b_f^2\left(\frac{\tau}{2} + \theta\right)^2 - b_f\left[2\left(s_l(t) - s_f(t) - \left(L_l + \Delta S^0\right)\right) - \dot{s}_f(t)\tau - \frac{\dot{s}_l^2(t)}{\hat{b}}\right]} \tag{3}$$

Steady-state solutions allow Wilson to derive a monotonically increasing speed–distance function for the general case of $b_f \neq \hat{b}$, which describes the equilibrium distance of the follower h_e:

$$\dot{s}_e(h_e) = \min\left[\begin{array}{c}0, \dfrac{\tau + \theta}{\dfrac{1}{|b_f|} - \dfrac{1}{|\hat{b}|}} \\ \cdot\left(-1 + \sqrt{1 + \dfrac{2\left(h_e - \left(L_l + \Delta S^0\right)\right)\left(\dfrac{1}{|b_f|} - \dfrac{1}{|\hat{b}|}\right)}{(\tau + \theta)^2}}\right), \dot{S}_f\end{array}\right] \tag{3a}$$

Then he first identifies a region of the space in which the speed–distance function is double valued. This condition occurs for the following parameter combinations:

$$\dot{S}_f \cdot \left(\frac{1}{|\hat{b}|} - \frac{1}{|b_f|}\right) - \tau - \theta > 0 \tag{4}$$

Equation 4 may hold only if $|\hat{b}| < |b_f|$. Then Wilson derives a condition for the linear instability of the model:

$$\theta < \dot{s}_f^* \cdot \left(\frac{1}{|\hat{b}|} - \frac{1}{|b_f|}\right) \tag{5}$$

Equation 5 may hold only if $|\hat{b}| > |b_f|$, that is, only when the follower underestimates the rate of braking of the vehicle ahead. $\dot{s}_f^* (< \dot{S}_f)$ represents the speed of the uniform flow. Equations 4 and 5 allow identifying a region of unstable uniform flow with a properly defined speed-headway function. This region is identified by the parameters satisfying the following system of inequalities:

$$\begin{cases}\dot{s}_f^* \cdot \left(\dfrac{1}{|\hat{b}|} - \dfrac{1}{|b_f|}\right) > \theta \\[3mm] \dot{S}_f \cdot \left(\dfrac{1}{|\hat{b}|} - \dfrac{1}{|b_f|}\right) \leq \tau + \theta\end{cases} \tag{6}$$

According to Wilson, this should be the condition for the Gipps' model to reproduce typical traffic mechanisms, such as flow breakdown and spontaneous traffic jam formation.

Following the work of Wilson, the derivation of the distance–speed function dual of the speed distance given by Equation 3a allowed Punzo and Tripodi to derive the macroscopic traffic flow models (i.e., the fundamental diagram) corresponding to the Gipps' microscopic equation, including an explicit formula for the flow at capacity (14). They extended the stationary models to the case of multiclass flows, also providing a framework for their calibration, that is, for the calibration of the Gipps' microscopic parameters based on average speeds and counts at detectors. This procedure was also applied by Ciuffo et al., who showed the potential benefits of using the calibrated parameters of the stationary speed–flow relationship as the starting point for the calibration of the traffic microsimulation model AIMSUN (which adopts a modified version of the Gipps' model, as already pointed out) (15).

Contemporary to the previous experiences, Rakha and Wang derived a procedure for the calibration of the Gipps' model based on its steady-state solution (16). No further description of such procedures will be made here since, for the lack of speed–flow data, their validity is not going to be tested in the current paper.

Further insights into the Gipps model were provided by Spyropoulou (8), who showed the speed–acceleration profile as defined by Equation 2a. Further details on this point will be provided in the next section. Gipps derived Equation 2a from empirical observation and therefore it is connected to the specific data he used for this purpose. Spyropoulou outlined that Equation 2b may lead to deceleration rates higher than those defined by the parameter b_f, in case the follower underestimated the braking capabilities of the leader (8). This property of the model was already mentioned by Gipps (1), it being clear to the author the difference between the b_f parameter (most severe braking that the driver of the following vehicle wishes to undertake) and the most severe braking that the driver of the following vehicle can undertake. This difference is not always clear among model users.

This condition can be easily proved by the following numerical example. Let a vehicle n travel at a constant maximum desired speed of 10 m/s and with an apparent reaction time $\tau_n = 1$ s. Let $b_n = -5$ m/s². At a certain instant t, the vehicle driver realizes that there is a fixed obstacle 5 m ahead and is forced to brake in order not to hit it. Applying Equation 2b, it may easily be seen that $\dot{s}_{f,\text{dec}}$ $(t + 1) = 0$. This formula means that the vehicle deceleration in the time interval $[t, t + 1]$ has been −10 m/s². This finding demonstrates that the parameter b_f cannot be taken directly from field data, as Gipps' initially supposed, but has to be calibrated together with the others by using a suitable optimization framework.

With Equation 3 the maximum deceleration allowed by the Gipps' model can be easily obtained. This deceleration is achieved when the vehicle traveling at maximum desired speed is forced to brake. The analytical limit for $\dot{s}_{f,\text{dec}}$ $(t + 1)$ is

$$b_f\left(\frac{\tau}{2} + \theta\right) < 0$$

In this case the maximum deceleration allowed by the model would be

$$-\frac{\dot{S}_f + \left|b_f\left(\frac{\tau}{2} + \theta\right)\right|}{\tau}$$

Actually, in common practice, the speed is set to be no lower than zero. Therefore, the practical maximum deceleration rate is just

$$|b_{f,\max}| = \frac{\dot{s}_f}{\tau} \tag{7}$$

Now the previous example is considered again. Let another vehicle $n1$ follow vehicle n at a constant speed of 10 m/s. The following assumptions are made: $\tau_{n1} = 1$ s, $b_{n1} = -8$ m/s², $\hat{b} = -5$ m/s² (correct estimation of the leader's braking rate). The distance at time t between the two vehicles, which allows both to proceed at constant speed, can be derived by the following equation proposed by Spyropoulou (8):

$$\dot{s}_{f,\text{const}}(t) = \frac{3b_f\tau + \sqrt{9b_f^2\tau^2 - 4b_f\left[2(\Delta S(t)) - \dfrac{\dot{s}_l^2(t)}{\hat{b}}\right]}}{2} \tag{8}$$

In the current case, the unknown quantity is $\Delta S(t)$ (representing the front-end distance between the two vehicles, comprehensive of the ΔS^0 term). Solving Equation 8, one has $\Delta S(t) = 11.25$ m. By applying Equation 2b iteratively, it can be shown that vehicle $n1$ comes to a safe stop in 4 s even if he underestimates the braking capabilities of the leader. Now the same experiment is repeated considering $b_{n1} = -12$ m/s². The result is that vehicle $n1$ intrudes on vehicle n after 2 s. The reason that this intrusion occurs is connected not only with the underestimate of the leader's actual braking capability but also with the difference between b_{n1} and $\hat{b}$, which makes the follower too confident of being able to safely brake in any situation. This well-known behavior of the Gipps' model poses serious concerns on the possibility of using the model for traffic simulation without introduction of appropriate control strategies.

In AIMSUN (17), the original Gipps' model is implemented (Equations 2a and 2b). The user is asked to choose among three versions of the car-following model. The different versions actually refer to different strategies for the selection of $\hat{b}$ (since it is not considered as an additional parameter). Different from the reality, the simulation environment knows the maximum deceleration rate parameter of each vehicle (regardless of its effect on the model, as previously mentioned). For this reason, in the first version of the model, the position expressed by Equation 9a is assumed:

$$\hat{b} = b_l \tag{9a}$$

$$\hat{b} = \frac{b_l + b_f}{2} \tag{9b}$$

$$\hat{b} = \vartheta \cdot b_f \tag{9c}$$

where ϑ is the "sensitivity factor."

This position should have always ensured the safe behavior of the model. However, for the reasons previously described, it does not prevent intrusions among vehicles. This outcome is the case also for the second version of the model (Equation 9b), even if it allows for more realistic distances to be kept among vehicles (17). The third version of the model is instead more in line with the original Gipps' formulation, with the parameter ϑ to be calibrated as it was for $\hat{b}$.

The third version of the model also introduces a minimum headway the follower wishes to undertake. This additional parameter introduces the following control strategy:

$$\text{if } \left\{\begin{matrix} \left[s_l(t+\tau) - \left(L_l + \Delta S^0\right)\right] \\ -\left[s_f(t) + \dot{s}_f(t+\tau) \cdot \tau\right] \end{matrix}\right\} < \dot{s}_f(t+\tau) \cdot \min H_f$$

$$\dot{s}_f(t+\tau) = \frac{\left[s_l(t+\tau) - \left(L_l + \Delta S^0\right)\right] - s_f(t)}{\min H_f + \tau} \quad (10)$$

end if

in which $\min H_f$ is the new parameter representing the minimum time headway to be kept between follower and leader. Though interesting, this solution modifies the dynamics described by the Gipps' model. The effect of such a modification should be analyzed.

Instead of this approach, it would be wise to have a relationship among the model parameters like those presented in Equations 4 and 5. Actually, even if Equation 4 was derived in a totally different case, Punzo and Ciuffo conjectured to use it to limit the domain space of the model parameters in order to reduce the probability of losing the real solution of the Gipps' model (a sort of similarity between the loss of global existence for the speed–flow diagram in stationary conditions and the intrusion between two vehicles in the car-following condition was assumed) (*18*). Numerical experiments using real trajectories for the leader vehicle provided good results, with no crash occurrence over hundreds of thousands of parameter combinations. However, by using Equation 4 to evaluate the two experiments previously described, it is possible to find that in both cases the condition expressed by Equation 4 is not satisfied and thus in both the cases, no crashes should have occurred. Thus, in principle it does not ensure that the model always provides real solutions. New perspectives on this issue have been recently opened by Wilson and Ward (*19*).

Integration Scheme and Boundary Conditions

The model in Equations 2 and 3 is a delayed differential equation (τ being the delay). In the Gipps original paper (*1*), the solution of Equation 1 is made simple by adopting an integration step just equal to the delay τ. A forward Euler method on acceleration (i.e., a trapezoidal integration scheme on speed) is adopted for the calculations. The same approach is usually applied in the common practice. In the following this integration scheme will be referred to as the "classic integration scheme."

In AIMSUN (*17*) a different approach is adopted. The integration step dt is a submultiple of the delay τ (up to a minimum of 0.1 s) and the Gipps' model is applied at each simulation step. The space traveled by the vehicle within its lane is calculated considering the speed constant over the integration step. This method allows for a more accurate solution of the system of differential difference equations that the model produces than the approach adopted by Gipps. At the same time, it reproduces a more efficient transportation system (since it is updated more frequently), and this feature has to be considered in the calibration and validation phase. In the following, this integration scheme will be referred to as the "continuous integration scheme."

Besides the loss of a real solution in the Gipps' model because of wrong parameter combinations, real solutions for the model need to be ensured at the beginning of the simulation. In fact, especially in the case of calibrating the model against real trajectory data, the first simulation steps are usually driven by the real boundary conditions (initial speed, initial spacing, etc.) rather than by the model and its parameters. For this reason, the domain of the parameters has to be further constrained by means of the following nonlinear condition:

$$b_f^2\left(\frac{\tau}{2}+\theta\right)^2 - b_f\left[\begin{array}{c}2\left(s_l(t=0) - s_f(t=0) - \left(L_l + \Delta S^0\right)\right)\\[4pt]-\dot{s}_f(t=0)\tau - \dfrac{\dot{s}_l^2(t=0)}{\hat{b}}\end{array}\right] \geq 0 \quad (11)$$

The constraint relates to the initial state of the simulation (i.e., at $t = 0$) to avoid the following vehicle's intruding on the effective size of the leader.

Acceleration Component of Gipps' Car-Following Model

The acceleration component of the Gipps' car-following model tries to resemble the behavior of a driver when the headway with the vehicle ahead is sufficiently large. As already pointed out, it was empirically derived by Gipps. For the sake of generality it is rewritten in the following way:

$$\dot{s}_{f,\text{acc}}(t+\tau) = \dot{s}_f(t) + \alpha \cdot \ddot{S}_f \cdot \tau \cdot \left(1 - \frac{\dot{s}_f(t)}{\dot{S}_f}\right) \cdot \left(\beta + \frac{\dot{s}_f(t)}{\dot{S}_f}\right)^{\gamma} \quad (12)$$

in which α, β, and γ are the parameters that, in the original formulation by Gipps (*1*), as well as in the literature, are assumed to be equal to 2.5, 0.025, and 0.5, respectively. From a modeling point of view, they are parameters like the others, and the authors want to understand how they affect the speed–acceleration relationship (also to understand if their calibration is necessary in order to improve model performance).

These values allow for $\ddot{S}_f$ to have the physical meaning of the maximum acceleration attained by the vehicle. This maximum acceleration is not attained in correspondence of $\dot{s}_f = 0$ but for $\dot{s}_f \cong 0.32 \cdot \dot{S}_f$ with the speed–acceleration profile reported in Figure 1*a*.

The speed–acceleration profile defined by the Gipps' model is quite different from real speed–acceleration profiles, in particular with regard to the necessity, in real driving, of shifting gears (see Figure 1*b*). The current authors claim that some improvements can be achieved by calibrating the α, β, and γ parameters (in particular because the maximum acceleration seems to arise for $\dot{s}_f = 0$ in real driving). As already pointed out, in order for $\ddot{S}_f$ to keep its physical meaning of maximum vehicle acceleration, the following condition must be imposed:

$$\max\left(\alpha \cdot \left(1 - \frac{\dot{s}_f(t)}{\dot{S}_f}\right) \cdot \left(\beta + \frac{\dot{s}_f(t)}{\dot{S}_f}\right)^{\gamma}\right) = 1 \quad (13)$$

It is assumed that

$$\frac{\dot{s}_f(t)}{\dot{S}_f} = x \quad (14a)$$

$$\alpha \cdot (1-x) \cdot (\beta + x)^{\gamma} = y \quad (14b)$$

Thus the condition in Equation 13 can be rewritten in the following form:

$$y\left(\frac{dy}{dx} = 0\right) = 1 \quad (15)$$

With a few algebraic manipulations,

$$\frac{dy}{dx} = 0 \Rightarrow x = \frac{\gamma - \beta}{1 + \gamma} \quad (16)$$

which implies that the relationship among α, β, and γ satisfying the condition in Equation 15 is the following:
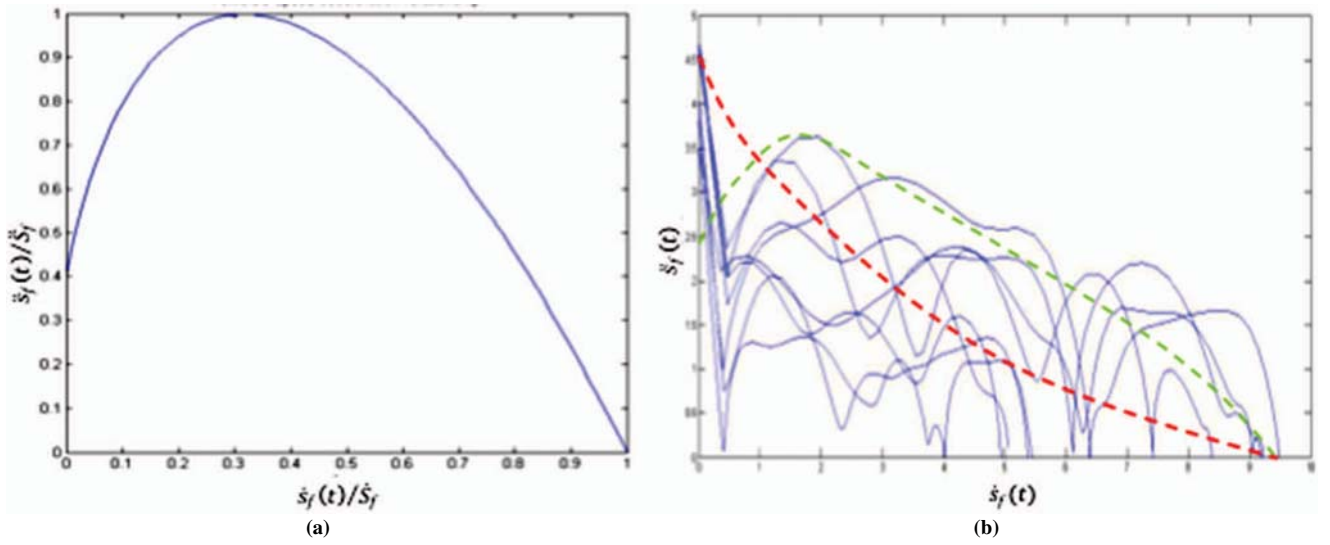
FIGURE 1 Speed–acceleration relationship (*a*) as defined by original formulation of Gipps' car-following model and (*b*) as retrieved from real trajectory (dashed lines are two hypothetical functions, which may resemble overall speed–acceleration profile).

$$\alpha \cdot \gamma^\gamma \cdot \left(\frac{1+\beta}{1+\gamma}\right)^{\gamma+1} = 1 \qquad (17)$$

α-γ-β combinations satisfying Equation 17 are reported in Figure 2*a*. Points lying on the surface depicted in the Figure 2*a* generate the speed–acceleration profiles drawn in Figure 2*b*.

From Figure 2*b* it is possible to note that some curves (those with γ < 1) achieve their maximum value for negative values of speed (all the curves in Figure 2*b* that do not show a maximum). In addition, by definition, Equation 17 does not allow speed–acceleration relationships to attain a maximum value greater than 1 for negative values of speed, which, however, in the domain [0,1] achieve $\ddot{s}_f(t) = \ddot{S}_f$ in correspondence with $\dddot{s}_f = 0$ (like relationships of Figure 2*f* for γ < 1), which is probably the preferred condition.

For these two reasons it was decided to numerically derive all the α, β, and γ parameter combinations satisfying the condition in Equation 13 for speed varying in the domain [0, $\dot{S}_f$].

The results of the analysis, carried out using 10^6 Monte Carlo samples, are shown in Figure 2*c*. The condition of Equation 13 is represented by the dots in Figure 2*c* lying on the surface of the separation between dark and light points. The corresponding speed–acceleration profiles are shown in Figure 2*d*. As opposed to the previous case, a wider variety of curves was found, depicting a higher number of possible speed–acceleration profiles.

In order to derive an analytical formulation of the surface interpolating the red dots of Figure 2*c*, a kriging approximation was derived from their coordinates by using the freely available MATLAB tool DACE (*20*). A description of the peculiarities of kriging metamodels is beyond the aims of the present paper. Further information can be found elsewhere (*21*).

The kriging metamodel was derived by using 2,500 points and describes the function α = *f*(β, γ) for the Gipps' model. In this way it is possible to calibrate the two parameters only, deriving α from the metamodel. As a result, Equation 12 can be rewritten in the following way:

$$\dot{s}_{f,acc}(t+\tau) = \dot{s}_f(t) + \alpha(\beta,\gamma) \cdot \ddot{S}_f \cdot \tau \cdot \left(1 - \frac{\dot{s}_f(t)}{\dot{S}_f}\right) \cdot \left(\beta + \frac{\dot{s}_f(t)}{\dot{S}_f}\right)^\gamma \qquad (18)$$

The kriging approximation of the function α = *f*(β, γ) is available at http://dl.dropbox.com/u/3874006/alfa2500.zip together with the instructions for its use.

To reduce the total number of parameters, the effect of considering α = 1 was studied. To this aim, the numerical study on the β and γ parameters only was repeated, finding the results showed in Figure 2, *e* and *f*. In Figure 2*e* the lighter dots represent the β-γ combinations for which Equation 13 is lower than 1, and the darker ones are those combinations for which Equation 13 is higher than 1, for α = 1. Points at the boundary between the four regions satisfy Equation 13. In particular, in correspondence with α = 1, when γ = 0, the condition is satisfied per each value of β. In addition, for γ < 1, the maximum acceleration is always in correspondence with $\dot{s}_f = 0$ and in this case β must always be equal to 1. For γ > 1, then, the relationship between β and γ is the theoretical one expressed by Equation 17 for α = 1. The β-γ relationship adopted here is graphically represented in Figure 2*e* with the solid black line. As can be seen from Figure 2*f*, the points lying along the chosen β(γ) relationship generate a wide variety of speed–acceleration profiles, even if not all those depicted in Figure 2*d* for the α(γ,β) function.

The mathematical formulation of the β(γ) function is therefore the following:

$$\begin{aligned} &\text{if } \gamma \leq 1 \Rightarrow \beta = 1 \\ &\text{if } \gamma > 1 \Rightarrow \beta = \frac{\gamma+1}{\gamma^{\frac{\gamma}{\gamma+1}}} - 1 \end{aligned} \qquad (19)$$

and Equation 18 can be rewritten as follows:

$$\dot{s}_{f,acc}(t+\tau) = \dot{s}_f(t) + \ddot{S}_f \cdot \tau \cdot \left(1 - \frac{\dot{s}_f(t)}{\dot{S}_f}\right) \cdot \left(\beta(\gamma) + \frac{\dot{s}_f(t)}{\dot{S}_f}\right)^\gamma \qquad (20)$$

In the next section the results of calibrating 10 versions of the Gipps' car-following model against two vehicle trajectories will be described.
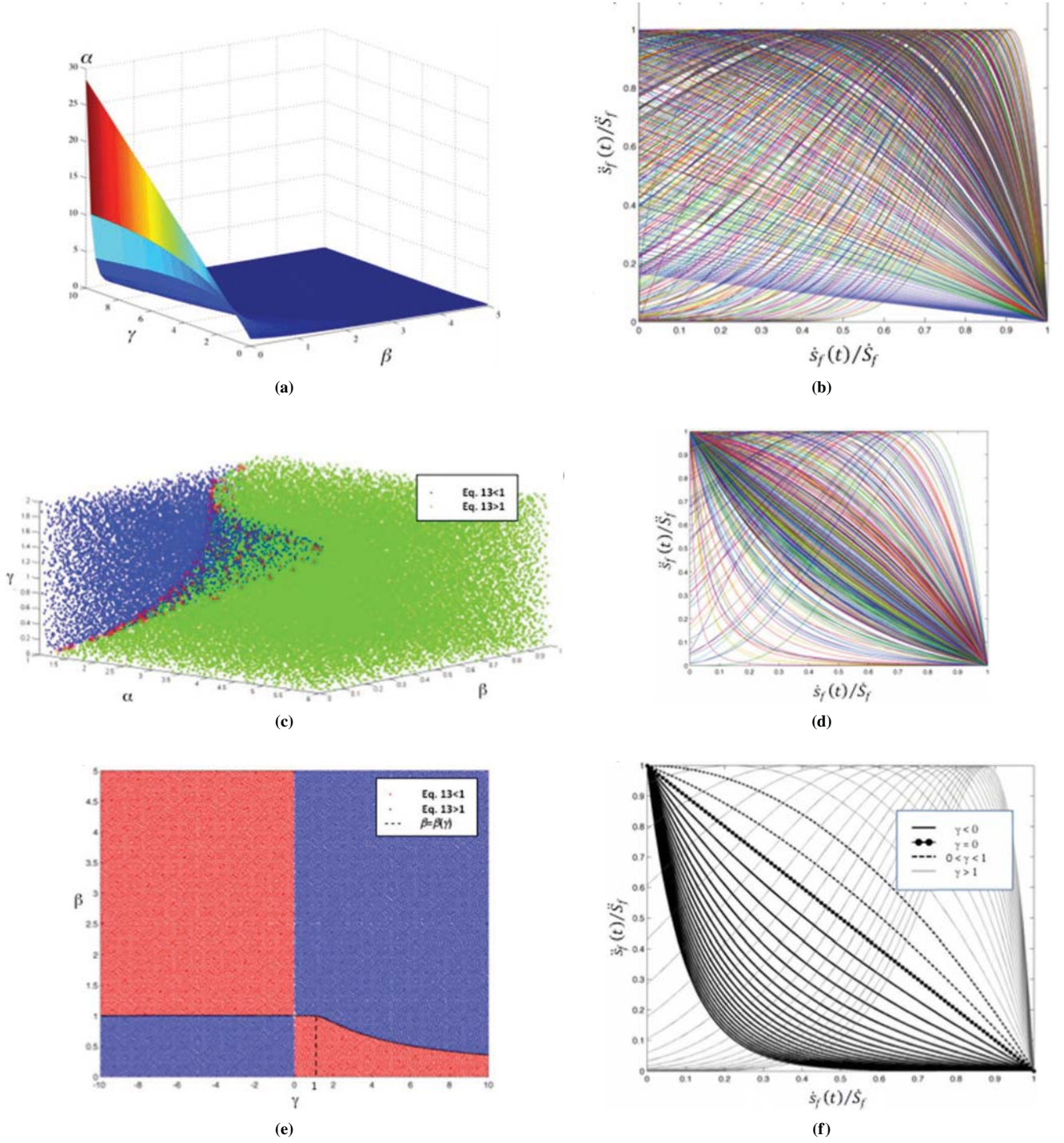
FIGURE 2 The α-β-γ relationships and corresponding speed–acceleration profiles allowed by Gipps' model: (*a*) α-β-γ relationship satisfying condition in Equation 17 and (*b*) corresponding speed–acceleration profiles; (*c*) α-β-γ relationship (surface that separates dark and light points) satisfying condition in Equation 13 and (*d*) corresponding speed–acceleration profiles; and (*e*) γ-β relationship (solid black line) of Equation 19 and (*f*) corresponding speed–acceleration profiles.

MODEL CALIBRATION AND VALIDATION AGAINST TRAJECTORY DATA

Now the differences among different versions of the Gipps' model in reproducing real vehicles' trajectories in car-following situations can be evaluated. Such trajectories were obtained from a series of car-following experiments carried out along roads in areas surrounding Naples, Italy, under real traffic conditions between October 2002 and July 2003. Experiments were performed by driving four vehicles in a platoon along urban and extraurban roads under different traffic conditions. All vehicles were equipped with kinematic differential Global Positioning System receivers that recorded the position of each vehicle at 0.1-s intervals. More details on data, including the description of data collection and the filter designed to process raw data, can be found elsewhere (*22, 23*).

Trajectory data used here are designated 30C and 30B. Set 30C is for a two-lane urban road (one lane per direction) and is 6 min long, and Set 30B is for a two-lane rural highway and is 4.2 min long (*22*). In this study the model is calibrated on trajectories of the first and the second vehicles of each platoon and validated on the trajectories of the others.

Formulation and Solution of Calibration Problem

Calibrating a simulation model consists of finding the values of its parameters that allow the model itself to reproduce in the best possible way the behavior of the real system simulated. It is equivalent to the solution of a constrained minimization problem in which the objective function expresses the deviation of the simulated measurements from those observed:

$$\min_{\beta, \gamma} f\left(M^{\text{obs}}, M^{\text{sim}}\right) \qquad (21)$$

possibly subject to the following constraints:

$$l_{\beta,i} \le \beta_i \le u_{\beta,i} \qquad i = 1 \dots m$$

$$l_{\gamma,j} \le \gamma_j \le u_{\gamma,j} \qquad j = 1 \dots n$$

and potentially also to other constraints:

$$g_k\left(\beta_i, \gamma_j\right)? b_k \qquad i = 1, \dots, m; j = 1, \dots, n; k = 1, \dots, l$$

where

β_i, γ_i = respectively, vectors of continuous and discrete model parameters, potentially belonging to m different classes of simulation subjects;

$f(\cdot)$ = objective function (or fitness or loss function) to be minimized, which measures distance between simulated and observed traffic measurements, M^{sim} and M^{obs};

$l_{\beta,i}, l_{\gamma,i}, u_{\beta,i}, u_{\gamma,i}$ = model parameter lower and upper bounds;

$g_k(\beta_i, \gamma_j)$ = scalar-valued linear or nonlinear function of model parameters β_i, γ_j that calculates left-hand side of kth constraint;

b_k = constant value equal to right-hand side of kth constraint; and

? = one of following relational operators: $\le\le$, $\ge$, or $==$.

The problem in Equation 21 cannot be solved analytically, since a simulation model is being dealt with. For this reason an optimization algorithm is used instead. In this case the Opt/Quest Multistart algorithm was used as implemented in the optimization package LINDO API (*24*). The good performance of this algorithm in dealing with similar problems has been tested in several studies [see, for example, work by Ciuffo et al. (*15, 25*)].

In this study, M^{sim} and M^{obs} are respectively the simulated and observed trajectory data. A trajectory is defined as the time series of the positions or the speeds assumed by a vehicle during its path. In order to compare simulated and observed trajectories an appropriate measure of goodness of fit is necessary. Ciuffo et al. have recently shown through an extensive experimental study that a car-following model should be calibrated by using the root square error of the time series of the vehicle's speeds (*26*). For this reason the same approach was adopted here.

Evaluated Versions of Gipps' Car-Following Model

Twenty calibration experiments were performed. In particular, five different versions of the Gipps' model were considered:

1. Original formulation (Equations 2*a*, 2*b*), six parameters (Original);
2. Original formulation with the AIMSUN control strategy on the minimum headway (Equation 10), seven parameters (Original AIMSUN);
3. Original formulation (without assuming that θ = τ/2, Equation 3) with the constraint of Equation 4 on the parameters, seven parameters (Original Wilson);
4. Modified acceleration function (Equation 20) and Equation 3 for the deceleration part of the model, eight parameters (Modified Version 1); and
5. Modified acceleration function (Equation 18) and Equation 3 for the deceleration part of the model, nine parameters (Modified Version 2).

Furthermore, both integration schemes presented earlier were tested, and all the calibrations for both the 30B and 30C data sets were repeated. From the analysis of the trajectories, the following values were considered for the parameters' upper (ub) and lower (lb) bounds reported in Table 1. Finally, in all the calibrations, the nonlinear constraint described in Equation 11 was adopted to deal with potential pitfalls at the beginning of the simulation.

RESULTS

The results of the calibration study are reported in Table 2 and Figure 3. In particular, in Table 2 the number of iterations required of the optimization algorithm to find the global minimum and the value of the objective function of the solution is reported. For the trajectory of both data sets, the minimum value of the root-mean-square error (*v*) is achieved by the modified Gipps' model reported (CalibID = 5) in Equations 18 and 3 for both integration schemes. The difference is, however, more significant for the trajectory in the 30C data set than that in the other data set. This finding is due to the fact that as the number and intensity of the acceleration phases increase, the influence of the acceleration component of the Gipps' model increases as well, and thus in these cases, the necessity for the calibration of the α, β, and γ parameters is confirmed.

TABLE 1 Lower and Upper Bounds for Parameters of Gipps' Model on Two Trajectory Data Sets

Parameter	30C lb	30C ub	30B lb	30B ub
$minH_f$	0	5	0	5
τ	0.1	1.0	0.1	1.0
β	0	5	0	5
γ	−4	4	−4	4
θ	0.05	0.5	0.05	0.5
$\dot{S}_f$	14.13	25	18.37	25
$\ddot{S}_f$	3.36	8	4.73	8
b_f	2	8	2	8
$\hat{b}$	2	8	2	8
ΔS^0	0.1	1.0	0.1	2.0

Table 2 also reports an additional measure of goodness of fit, defined as the sum of Theil's inequality coefficients calculated over the time series of both speed and vehicle spacing. This measure is important in order to understand how well the simulated trajectory matches the real one for both the speed and the distance between leader and follower. A further discussion of this goodness of fit can be found elsewhere (*26*).

Finally, Table 2 reports the values of the calibrated parameters. The parameter values obtained for Version 2 of the Gipps' model (referred to as the AIMSUN version and described by Equation 10) always violate the condition of Equation 4. In this case the Gipps' model would provide a double-valued speed–flow diagram in the hypothesis of uniform flow. However, the introduction of the minimum headway parameter considerably changes the model structure, and therefore this parameter cannot be easily assessed. On the contrary, all the other parameter combinations satisfy Equation 4.

The same results are then also graphically reproduced in Figure 3. In particular, Figure 3, *a* and *b,* show the value attained by the Theil's inequality coefficient in the different calibrations. The modified version of the Gipps' model (Equations 18 and 3) clearly outperforms the other versions for the trajectory of Data Set 30C, whereas in the other case, all the versions have approximately the same performance. The integration scheme does not seem to have a significant impact on the calibrated trajectory. Figure 3, *c* and *d,* instead, show the efforts in terms of algorithm iterations to find the global solution of the calibration problem. In this case, the Gipps' modified version requires more algorithm iterations than all the other versions to be calibrated. The other modified version (CalibID = 4) instead slightly improves the performance of the calibrated model without affecting the number of algorithm iterations that much. Again, the effect of the integration scheme does not appear to influence the overall model behavior.

All these considerations, however, have to be further confirmed by validating the model. Indeed, since the different versions of the Gipps' model consider different numbers of parameters, the improve-

TABLE 2 Calibration Results of Different Versions of Gipps' Car-Following Model

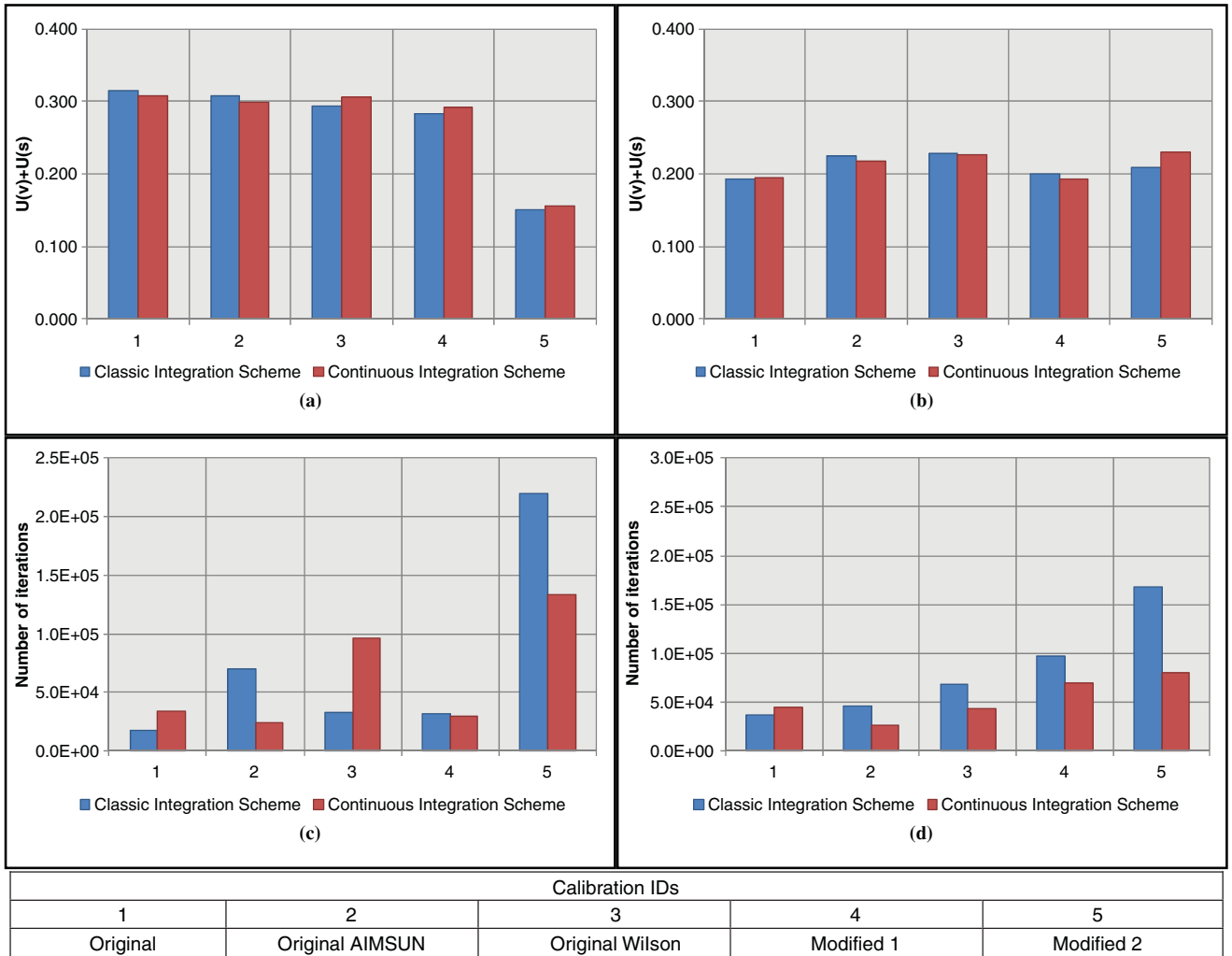| CalibID	Iterations	RMSE(v)	U(v) + U(s)	α	β	γ	τ	θ	$\dot{S}_f$	$\ddot{S}_f$	ΔS^0	$\hat{b}$	b_f	min H_f
Trajectory Data Set 30C: Classic Integration Scheme														
1	18,150	0.650	0.316	2.50	0.03	0.50	0.60	0.30	19.25	7.02	1.00	8.00	5.62	—
2	69,607	0.630	0.307	2.50	0.03	0.50	1.00	0.50	25.00	3.36	0.96	2.00	3.14	1.12
3	32,955	0.617	0.294	2.50	0.03	0.50	0.80	0.05	14.13	3.36	0.67	8.00	5.59	—
4	31,663	0.664	0.283	1.00	0.67	3.78	0.30	0.10	14.13	8.00	1.00	8.00	4.06	—
5	219,435	0.480	0.151	0.27	0.00	−0.17	0.20	0.34	24.39	3.36	1.00	8.00	6.28	—
Trajectory Data Set 30C: Continuous Integration Scheme														
1	33,638	0.647	0.308	2.50	0.03	0.50	0.60	0.30	14.13	3.36	1.00	8.00	5.80	—
2	23,956	0.628	0.300	2.50	0.03	0.50	0.90	0.45	14.13	3.36	0.95	2.00	2.82	1.10
3	96,582	0.627	0.305	2.50	0.03	0.50	0.80	0.05	25.00	3.36	0.70	8.00	5.35	—
4	29,580	0.646	0.292	1.00	0.99	1.19	0.50	0.05	24.38	3.37	1.00	8.00	4.41	—
5	133,536	0.453	0.156	0.27	0.00	−0.19	0.70	0.05	25.00	3.36	0.85	4.71	4.73	—
Trajectory Data Set 30B: Classic Integration Scheme														
1	36,410	0.531	0.193	2.50	0.03	0.50	0.20	0.10	25.00	4.73	2.00	8.00	4.93	—
2	46,611	0.458	0.224	2.50	0.03	0.50	1.00	0.50	23.87	7.34	2.00	2.00	3.40	0.93
3	68,195	0.470	0.228	2.50	0.03	0.50	1.00	0.05	24.25	8.00	2.00	4.60	4.97	—
4	97,532	0.494	0.201	1.00	0.02	0.00	0.30	0.50	18.37	4.73	2.00	8.00	7.37	—
5	168,382	0.419	0.209	0.19	0.04	−0.49	1.00	0.07	20.62	4.73	2.00	6.05	8.00	—
Trajectory Data Set 30B: Continuous Integration Scheme														
1	44,227	0.553	0.195	2.50	0.03	0.50	0.10	0.05	19.30	7.58	2.00	8.00	4.49	—
2	26,291	0.459	0.217	2.50	0.03	0.50	0.80	0.40	20.33	7.18	2.00	2.00	7.44	0.92
3	43,212	0.480	0.227	2.50	0.03	0.50	0.70	0.23	21.88	7.67	2.00	8.00	7.89	—
4	69,839	0.519	0.192	1.00	−1.15	−1.80	0.10	0.50	24.65	5.67	2.00	8.00	6.20	—
5	79,603	0.436	0.230	0.11	0.01	−0.45	1.00	0.25	20.67	8.00	2.00	5.29	7.77	—

FIGURE 3 Calibration results of versions of Gipps' car-following model: (a, b) differences in terms of Theil's inequality coefficient and (c, d) number of iterations (calibration IDs refer to versions of model listed in section on evaluated versions of Gipps' car-following model).

ments in the performance of those versions with more parameters (CalibID = 4, 5) might be due to their overfitting capabilities rather than to their improved predictive power.

The validation of the 20 calibrated models is presented in the next section.
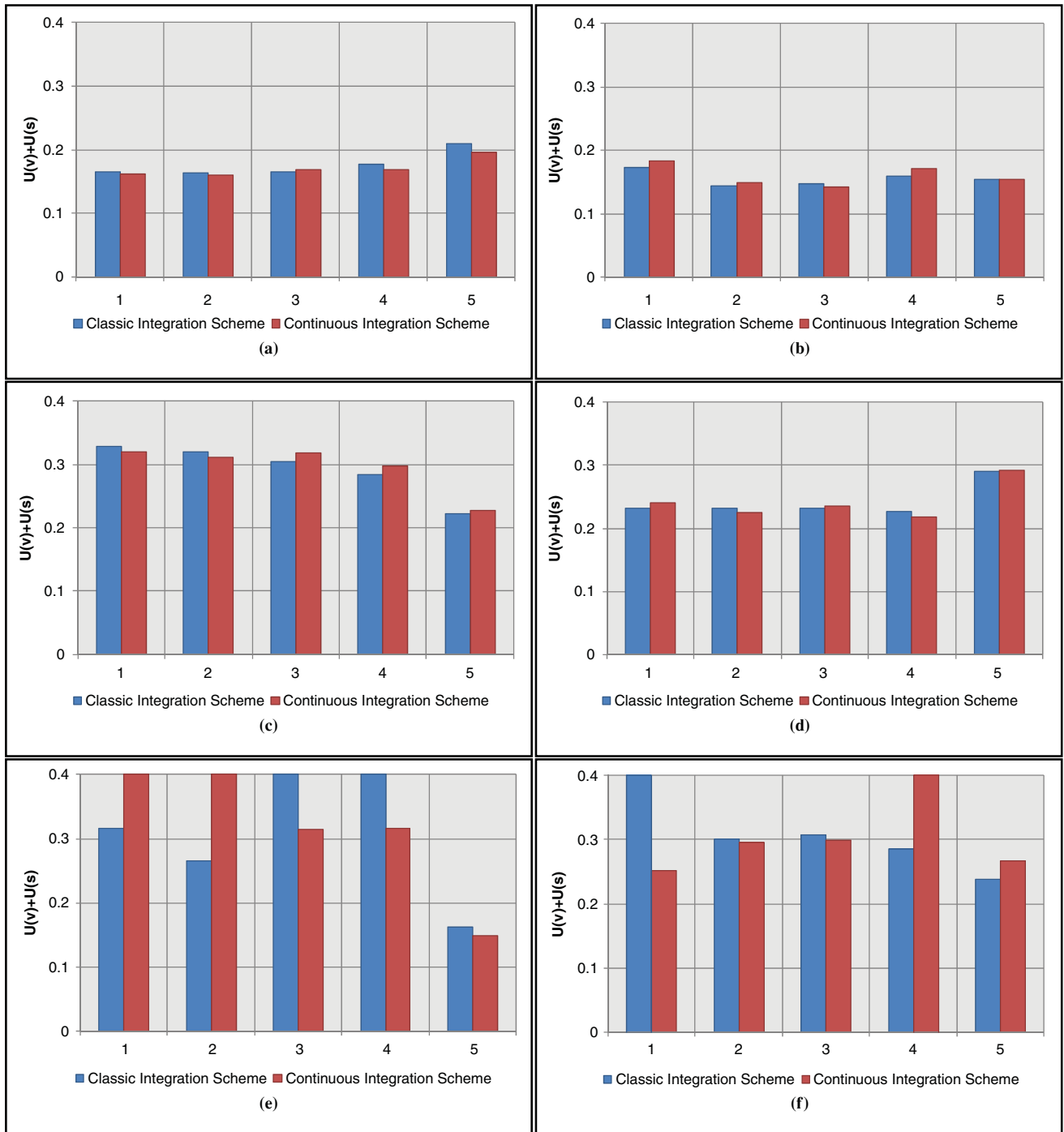
MODEL VALIDATION

Validating a car-following model consists of verifying that the model calibrated on the basis of a specific trajectory is able to reproduce another trajectory collected in a different moment or in a different place (*23*). Since the two data sets 30B and 30C consist of the trajectories of the same drivers traveling in the same order along different stretches of roads in different moments, and since the models were calibrated on the trajectories of the first two vehicles of the platoons only, it was decided to validate the models either on the trajectories of the other vehicles of the same platoon or on the trajectories of the same vehicles in the other platoon. Practically speaking, trajectories validated on the first two trajectories of Data Set 30B were validated both on trajectories of the third and fourth vehicle of Data Set 30B and on the trajectories of the first two vehicles in Data Set 30C.

Results are shown in Figure 4. Figure 4, *a, c,* and *e* refer to the validation of the models calibrated on trajectories pertaining to Data Set 30C. It is possible to see that the trajectory of the third vehicle is well depicted by all the model versions. Errors on the fourth trajectory start to increase approximately with the same magnitude for all the models. Errors on the second trajectory of the other data set considerably increase but for the modified Gipps' model (CalibID = 5), especially for the version calibrated on Data Set 30C. This finding further confirms that as the number and intensity of the acceleration phases increase, the necessity to fine-tune the corresponding parameters also increases. This finding has a considerable effect also using the model with a lower number of accelerations (see Figure 4*e,* referring to the capabilities of the models calibrated on Data Set 30C to reproduce trajectories in 30B).

Again the effect of the integration scheme appears difficult to assess.

CONCLUSIONS

Car-following models are widely used by researchers and practitioners for road traffic studies. Although dozens of them have been presented so far, the model proposed by Gipps (*1*) is still one of

Calibration IDs				
1	2	3	4	5
Original	Original AIMSUN	Original Wilson	Modified 1	Modified 2

FIGURE 4 Validation results of versions of Gipps' car-following model: (*a*, *c*, *e*), validation of model versions calibrated on trajectory Data Set 30C and (*a*, *c*, *f*) those calibrated on trajectory Data Set 30B (*b*, *d*, *f*) (calibration IDs refer to different versions of model listed in section on evaluated versions of Gipps' car-following model).

the most extensively used. However, many features of the model are still somewhat unknown or neglected in common applications.

In this context, the current study summarizes and analyzes the main findings available in the scientific literature for the Gipps' car-following model and introduces some novel features of the same model that may improve its capability to reproduce real trajectory data.

In particular the structure of the acceleration component of the model is analytically investigated for the meaning of parameters α, β, and γ, which in the original formulation, as well as in common practice, are usually kept to the empirically derived values of 2.5, 0.025, and 0.5. Different possible versions of the Gipps' model are presented as they are derived from work by Wilson (5) and by Punzo and Tripodi (14), the implementation in the AIMSUN commercial package, and the modified versions presented in this paper. Their ability to accurately reproduce real trajectories is then evaluated and compared.

Results show that improved performance is only achieved via the calibration of all the previously mentioned α, β, and γ parameters. In particular the parameters considerably improve the model's predictive capability with well-resembling trajectories showing significant acceleration phases. This finding was expected since they describe the relationship between speed and acceleration during the vehicle acceleration phases.

ACKNOWLEDGMENTS

REFERENCES

1. Gipps, P. G. A Behavioural Car-Following Model for Computer Simulation. *Transportation Research Part B,* Vol. 15, No. 2, 1981, pp. 105–111.
2. Brackstone, M., and M. McDonald. Car-following: A Historical Review. *Transportation Research Part F,* Vol. 2, No. 4, 1999, pp. 181–196.
3. Helbing, D. Traffic and Related Self-Driven Many-Particles Systems. *Reviews of Modern Physics,* Vol. 73, 2001, pp. 1067–1139.
4. Cao, B., and Z. Yang. Car-Following Models Study Progress. KAM Proc., 2009 Second International Symposium on Knowledge Acquisition and Modeling, IEEE Computer Society, Washington, D.C., 2009. DOI 10.1109/KAM.2009.83.
5. Wilson, R. E. An Analysis of Gipps' Car-following Model of Highway Traffic. *IMA Journal of Applied Mathematics,* Vol. 66, 2001, pp. 509–537.
6. Bando, M., K. Hasebe, K. Nakanishi, A. Nakayama, A. Shibata, and Y. Sugiyama. Dynamical Model of Traffic Congestion and Numerical Simulation. *Physical Review E,* Vol. 51, 1995, pp. 1035–1042.
7. Ranjitkar, P., T. Nakatsuji, and A. Kawamura. Car-following Models: An Experiment Based Benchmarking. *Journal of the Eastern Asia Society for Transportation Studies,* Vol. 6, 2005, pp. 1582–1596.
8. Spyropoulou, I. Simulation Using Gipps' Car-following Model: An In-depth Analysis. *Transportmetrica,* Vol. 3, No. 3, 2007, pp. 231–245.
9. Barceló, J. Dynamic Network Simulation with AIMSUN. Proc., International Symposium on Transport Simulation, Yokohama, Japan, Kluwer Academic Publishers, Aug. 2002.
10. Liu, R. Traffic Simulation with DRACULA. In *Fundamentals of Traffic Simulation* (J. Barceló, ed.), Springer, 2010.
11. *SISTM: A Motorway Simulation Model.* U.K. Transport Research Laboratory, 1993. Leaflet, pp. LF2061.
12. Silcock, J. P. *SIGSIM version 1.0 users guide.* Working Paper. Centre for Transport Studies, University of London, 1993.
13. Hidas, P. A Car-following Model for Urban Traffic Simulation. *Traffic Engineering and Control,* Vol. 39, 1998, pp. 300–305.
14. Punzo, V., and A. Tripodi. Steady-State Solutions and Multiclass Calibration of Gipps' Microscopic Traffic Flow Model. In *Transportation Research Record: Journal of the Transportation Research Board, No. 1999,* Transportation Research Board of the National Academies, Washington, D.C., 2007, pp. 104–114.
15. Ciuffo, B., V. Punzo, and V. Torrieri. Comparison of Simulation-Based and Model-Based Calibrations of Traffic Flow Microsimulation Models. In *Transportation Research Record: Journal of the Transportation Research Board, No. 2088,* Transportation Research Board of the National Academies, Washington, D.C., 2008, pp. 36–44.
16. Rakha, H. A., and W. Wang. Procedure for Calibrating Gipps' Car-Following Model. In *Transportation Research Record: Journal of the Transportation Research Board, No. 2124,* Transportation Research Board of the National Academies, Washington, D.C., 2009, pp. 113–124.
17. *Aimsun 6.1 User's Manual: Microsimulator and Mesosimulator.* TSS–Transport Simulation Systems, Barcelona, Spain, 2010.
18. Punzo, V., and B. Ciuffo. Sensitivity Analysis of Car-Following Model: Methodology and Application. Presented at 90th Annual Meeting of the Transportation Research Board, Washington, D.C., 2011.
19. Wilson, R. E., and J. A. Ward. Car-following Models: Fifty Years of Linear Stability Analysis: A Mathematical Perspective. *Transportation Planning and Technology,* Vol. 34, No. 1, 2011, pp. 3–18.
20. Lophanev, S. N., H. B. Nielsen, and J. Sondergaard. *DACE: A Matlab Kriging Toolbox, version 2.0.* IMM Technical Report IMM-REP-2002-12. Technical University of Denmark, Lyngby, 2002.
21. Kleijnen, J. P. C. *Design and Analysis of Simulation Experiment.* International Series in Operations Research and Management Science. Springer, Stanford, Calif., 2008.
22. Punzo, V., D. J. Formisano, and V. Torrieri. Nonstationary Kalman Filter for Estimation of Accurate and Consistent Car-Following Data. In *Transportation Research Record: Journal of the Transportation Research Board, No. 1934,* Transportation Research Board of the National Academies, Washington, D.C., 2005, pp. 3–12.
23. Punzo, V., and F. Simonelli. Analysis and Comparison of Microscopic Traffic Flow Models with Real Traffic Microscopic Data. In *Transportation Research Record: Journal of the Transportation Research Board, No. 1934,* Transportation Research Board of the National Academies, Washington, D.C., 2005, pp. 53–63.
24. *LINDO API User Manual 2.0.* LINDO Systems, Inc., Chicago, Ill., 2003.
25. Ciuffo, B., V. Punzo, and E. Quaglietta. Kriging Meta-Modelling to Verify Traffic Microsimulation Calibration Methods. Presented at 90th Annual Meeting of the Transportation Research Board, Washington, D.C., 2011.
26. Ciuffo, B., V. Punzo, and M. Montanino. *The Calibration of Traffic Simulation Models: Report on the Assessment of Different Goodness of Fit Measures and Optimization Algorithms MULTITUDE Project–COST Action TU0903.* JRC68403. Joint Research Centre, European Commission, Brussels, Belgium, 2012. ISBN 978-92-79-22812-4. http://publications.jrc.ec.europa.eu/repository/handle/111111111/23638.